Holographic equilibration in confining gauge theories under external magnetic fields

T. Demircik,^a U. Gürsoy,^b

^a Faculty of Engineering and Natural Science, Sabanci University, Tuzla, Istanbul, 34956, Turkey
 ^b Institute for Theoretical Physics and Center for Extreme Matter and Emergent Phenomena,
 Utrecht University, Leuvenlaan 4, 3584 CE Utrecht, The Netherlands

E-mail: tunad@sabanciuniv.edu, u.gursoy@uu.nl

ABSTRACT: We investigate the effect of external magnetic fields on equilibration in the improved holographic QCD theory in the deconfined phase using the AdS/CFT correspondence. In particular we calculate the quasinormal mode spectra in the corresponding black brane solutions and study their dependence on temperature, momentum and magnetic field, both in the scalar and the shear channels. We find complex patterns in the motion of quasinormal modes on the complex plane, including certain cross overs between the lowest lying modes under varying momentum.

Keywords: AdS/CFT, Holographic QCD, Quasinormal modes, Thermalization

ARXIV EPRINT: 16-.—-

C	ontents	
1	Introduction and summary	1
2	Gravity setting	4
	2.1 The glue sector	4
	2.2 The flavor sector	4
	2.3 Background at a finite magnetic field and temperature	6
3	Quasinormal mode spectra	8
	3.1 Scalar channel	9
	3.2 Shear channel	12
4	Discussion	14
A	Coefficients in the gauge invariant variable equations of the shear channel	17

1 Introduction and summary

Quantum Chromodynamics exhibits a host of interesting phenomena when put under a strong external magnetic field B. They range from a complicated dependence of the quark condensate on B, resulting in phenomena such as magnetic catalysis [1], inverse magnetic catalysis [2], to the existence of new anomalous transport properties resulting in the chiral magnetic and vortical effects, the chiral magnetic wave [3, 4] and production of electric currents as a result of Faraday and Hall effects [5]. Dependence of finite temperature QCD dynamics on magnetic fields are not only of academic interest, as there is a significant possibility of observing the associated phenomena in the non-central heavy ion collision experiments. It is known that rather large magnetic fields are produced by the spectator ions in such non-central collisions [2, 3, 5-10]. Many of these estimations predict presence of these magnetic fields even after the formation of the Quark-Gluon Plasma in such experiments. Therefore, it is crucial to understand the effects of magnetic fields on the dynamics of the quark-gluon plasma. See [11] for an extensive review of phenomena associated to presence of magnetic fields. There are also multiple indications that the QGP produced in these experiments is strongly interacting [12] preventing a direct study in perturbative QCD.

Together with the lattice and hydrodynamic simulations, the AdS/CFT correspondence [13–15] is established as an alternative non-perturbative tool in studying such phenomena in QCD-like *confining* gauge theories [16–22]. Recently the AdS/CFT studies have also led to many new insights in regard to non-equilibrium, real-time physics [23–26]. Since such real-time problems are hard to study with lattice methods, the non-perturbative

tools provided by the AdS/CFT correspondence becomes especially important in this respect. Equilibration of small fluctuations around a system at hydrodynamic equilibrium is generically determined by the poles of the associated retarded Green functions on the complex plane. In the dual holographic description they correspond to the quasinormal mode (QNM) spectrum of bulk fluctuations on the corresponding black-brane background. These modes can be obtained by studying fluctuations in the bulk, with infalling boundary conditions on the horizon and vanishing Dirichlet boundary conditions near the asymptotically AdS boundary [27].

In this paper, we take the first step to study holographic equilibration in QCD-like confining gauge theories under external magnetic fields. QNMs in the context of holography has been studied extensively, see [28] for a review. Such studies in the case of realistic, QCD-like confining theories have only recently started to appear [29–34]. QNMs in systems with magnetic fields have also been studied in the context of holography before, see for example [35] but, to our knowledge, the problem has not been investigated in the literature in the backgrounds corresponding to confining gauge theories with magnetic fields. For the gravity background we consider the bottom-up holographic models first considered in [22, 36–38]. These models, that are called the *improved holographic QCD* (ihQCD) provide a realistic description of the particle spectrum in the low temperature phase, the confinement-deconfinement transition and the thermodynamic properties of QCD in the high temperature phase.

The ihQCD model has been extended to include the flavor sector in the large flavor number N_f , large color N_c (Veneziano) limit in [39–46]. We shall deal with such extended models, for the obvious reason that the magnetic field couples directly to the flavor sector, and only indirectly to the glue sector. The model contains two sectors. The glue sector is described by gravity in 5D coupled to a dilaton field that corresponds to the $\mathbb{T}rF^2$ operator. Running of the dilaton field in the holographic direction mimics the RG running of the 't Hooft coupling constant in energy. Secondly, there is the DBI flavor brane sector describing the dynamics of open strings on the glue background. End points of such open strings correspond to the quarks and anti-quarks on the dual theory. The lowest lying excitation, the open string tachyon field corresponds to the quark condensate [36, 39, 41]. Finally there is a bulk gauge field on the flavor branes that is chosen such that it corresponds to the magnetic field on the dual field theory. The background we consider in this paper is, then, an asymptotically AdS black-brane solution with an anisotropy in the direction along the magnetic field that is coupled to the bulk gauge field and the aforementioned tachyon field. When the magnetic field is set to zero, the gravitational theory exhibits a first order Hawking-Page [47] type phase transition [37, 41]. This phase transition corresponds to the confinement-deconfinement transition in the dual confining gauge theory. The phase transition continues to exist when the magnetic field is turned on, however the value of the transition temperature T_c shifts with B [48, 49]. As we are interested in equilibration in the deconfined phase of the gauge theory, we consider QNMs in the black brane phase, that is for temperatures $T > T_c^{-1}$.

¹The black brane solutions in the improved holographic QCD models exist above a certain minimum

One can think of the spectrum of QNMs in the presence of magnetic fields as analogs of the Landau levels in the deconfined phase of the confining gauge theory. We calculate the QNM spectrum on this black-brane by numerically solving the fluctuations that correspond to the *shear* and the *scalar* modes. We consider the few lowest lying modes at finite momentum \vec{k} , that we take parallel to the magnetic field \vec{B} for simplicity², and study their dependence on B, k and temperature T. Various interesting phenomena arise from our studies:

- We observe two distinct classes of QNMs. Firstly there is a class of QNMs that possess both imaginary and real parts. Secondly there is a QNM that is purely imaginary and remains purely imaginary for any value of B, T and k. This kind of purely imaginary QNMs were observed before in electrically charged AdS-RN black brane solutions, see for example [35, 50]. However, the latter paper does not report any QNMs of this type in magnetically charged black brane solutions [51] whereas we find an example of such modes here. Whether this mode is a part of series of infinitely many purely imaginary QNMs, as in [50] remains to be seen. In our studies we were able to find only one such example.
- The absolute values of the imaginary parts of QNMs increase with increasing magnetic field, as also observed in [35] before. This is shown in figures 2 and 5 for the scalar and the shear channels respectively. This is in complete analogy with the situation in the vacuum state, where the Landau levels also increase with B. This has an important implication for the equilibration process in the presence of magnetic fields. Since the equilibration time is inversely proportional to the imaginary part of the quasinormal modes, $\tau \sim -1/\mathrm{Im}\omega$, larger B implies shorter equilibration times. The only exception is purely imaginary mode in the scalar chanel which is shown in figure 2(c).
- The motion of QNMs with changing momentum exhibit crossing phenomena. In particular, we observe that the imaginary part of the QNMs both in the scalar and the shear channels cross as k increases, see figures 3(b) and 6(b) respectively. This means that the dominant mode that controls the equilibration process depends on the value of k.

The rest of the paper is organized as follows. In the next section we present our 5D gravity set-up and the black brane background in detail. Section 3 contains our main studies of the quasinormal mode spectra. In the last section 4 we discuss our findings and their interpretation from the point of view of the boundary gauge theory. Appendix A detail our calculations.

Note added: In the first version of this paper we reported an instability that appeared for large values of momentum. This turned out to be due to an error in our code that we fixed in this version and we do not find any perturbative instability in the system.

temperature $T_{min} < T_c$. Therefore, one may also study the QNMs in the range $T_{min} < T < T_c$. These solutions were argued to correspond to a supercooled phase of the theory in [29] and a study of the QNMs for B = 0 was presented in this paper.

²Otherwise decomposition of these fields under Lorentz little group becomes complicated.

2 Gravity setting

The ihQCD [22, 36–38] is a string theory inspired bottom up holographic model that describes the glue sector of QCD-like confining gauge theories at large- N_c and large 't Hooft coupling. At high temperatures $T > T_c$, the model gives a realistic description of the glue plasma. In this paper we are interested in the effects of the magnetic field in the holographic description of the Quark-Gluon Plasma. Since the magnetic field couples the QGP through the flavor sector, i.e. the quarks, one first needs to add the flavor sector in the ihQCD theory. This can be achieved by considering N_f pairs of flavor branes and anti-branes embedded in the glue background. Let us denote the gravitational action corresponding to the glue and the flavor sectors by S_g and S_f respectively. The total gravitational action is

$$S = S_g + S_f. (2.1)$$

Since we are after non-negligible effects of the magnetic field on the QGP then the flavor sector should be taken as the same order as the glue. On the large N_c field theory side, this is achieved by considering the Veneziano limit, $N_f \to \infty$, $N_c \to \infty$ and $N_f/N_c = x$ =finite and $\lambda = g^2 N_c$ =fixed. We consider finite but small x, in practice we shall take x = 0.1. On the gravity side, finite x means taking into account the backreaction of the flavor sector on the glue background. The latter holographic theory was first constructed in [39–46] and called the holographic Veneziano QCD model, V-QCD for short. This is the model we use in this work.

2.1 The glue sector

The glue sector is described by the two-derivative Einstein-dilaton action [22, 36–38]

$$S_g = M_p^3 N_c^2 \int d^5 x \sqrt{-g} \left(R - \frac{4}{3} (\partial \phi)^2 + V_g(\phi) \right), \tag{2.2}$$

where M_p is the 5D Planck mass fixed by matching the high temperature limit of non-interacting fermions and bosons [42], $(Ml)^3 = (1 + 7x/4)/45\pi^2$, where l is the AdS radius. The metric is dual to the energy momentum tensor and the dilaton corresponds to the $\mathbb{T}rF^2$ operator in the boundary field theory. We further define

$$\lambda = e^{\phi} \,, \tag{2.3}$$

for notational convenience. This is identified with the 't Hooft coupling in the ihQCD theory.

2.2 The flavor sector

The flavor action is described by the generalized DBI action [39, 41] describing the embedding of the flavor branes

$$S_f = -\frac{1}{2} M_p^3 N_c \operatorname{Tr} \int d^5 x \left(V_f(\lambda, T^{\dagger} T) \sqrt{-\det \mathbf{A}_L} + V_f((\lambda, T T^{\dagger}) \sqrt{-\det \mathbf{A}_R} \right), \quad (2.4)$$

where

$$\mathbf{A}_{L\mu\nu} = g_{\mu\nu} + w(\lambda, T) F_{\mu\nu}^{L} + \frac{\kappa(\lambda, T)}{2} \left[(D_{\mu}T)^{\dagger} (D_{\nu}T) + (D_{\nu}T)^{\dagger} (D_{\mu}T) \right],$$

$$\mathbf{A}_{R\mu\nu} = g_{\mu\nu} + w(\lambda, T) F_{\mu\nu}^{R} + \frac{\kappa(\lambda, T)}{2} \left[(D_{\mu}T) (D_{\nu}T)^{\dagger} + (D_{\nu}T) (D_{\mu}T)^{\dagger} \right], \qquad (2.5)$$

and the covariant derivative is given by

$$D_{\mu}T = \partial_{\mu}T + iTA_{\mu}^{L} - iA_{\mu}^{R}T. \tag{2.6}$$

Here, A_L and A_R denote the gauge fields living on the flavor D-branes corresponding to the global flavor symmetry $U(N_f)_L \times U(N_f)_R$ on the dual field theory. T is a complex scalar, the open string tachyon, which transforms as a bifundamental under this flavor symmetry and corresponds to the quark mass operator. The vector and the axial combinations are given by

$$V_{\mu} = \frac{A_{\mu}^{L} + A_{\mu}^{R}}{2}$$
 , $A_{\mu} = \frac{A_{\mu}^{L} - A_{\mu}^{R}}{2}$. (2.7)

Following [41] we choose the tachyon potential as

$$V_f(\lambda, TT^{\dagger}) = V_{f0}(\lambda)e^{-a(\lambda)TT^{\dagger}}.$$
 (2.8)

We also make a simplifying assumption and take $\kappa(\lambda, T)$ and $w(\lambda, T)$ independent of T. The potentials $V_{f0}(\lambda)$, $a(\lambda)$, $\kappa(\lambda)$ and $w(\lambda)$ are constrained by requirements from the low energy QCD phenomenology, such as chiral symmetry breaking and meson spectra [44].

We make a final simplification by choosing a diagonal tachyon field

$$T = \tau(r) \mathbb{I}_{N_f},\tag{2.9}$$

that corresponds to N_f light quarks with the same mass in boundary field theory. Holographically, $\tau(r)$ is dual to the quark mass operator and its non-trivial profile is responsible for the chiral symmetry breaking on the boundary theory. As mentioned above, we consider small values of the parameter $x = N_f/N_c$ in this work, for which the presence of the magnetic field is not expected to change the phase structure substantially. Therefore the dominant phase should be deconfined and chirally symmetric ($\tau(r) = 0$) at high temperatures. For relatively small values of the magnetic field, the flavor action (2.4) can be expanded as

$$S_f = -M_p^3 N_c \operatorname{Tr} \int dx^5 V_f(\lambda) \sqrt{-g} \sqrt{\det(\delta_\nu^\mu + w(\lambda)^2 g^{\mu\rho} F_{\rho\nu})}$$
$$= -M_p^3 N_c N_f \int dx^5 V_f(\lambda) \sqrt{-g} \left(1 + \frac{w(\lambda)^2}{4} F_{\mu\nu} F^{\mu\nu} \right). \tag{2.10}$$

where $F_{\mu\nu}$ is the field strength corresponding to V_{μ} in (2.7).

2.3 Background at a finite magnetic field and temperature

Our complete action is given by (2.2) and (2.10). The background solution we seek should solve the Einstein, the dilaton and the Maxwell equations

$$R_{\mu\nu} - \frac{1}{2}g_{\mu\nu}R - \left(\frac{4}{3}\partial_{\mu}\phi\partial_{\nu}\phi - \frac{2}{3}g_{\mu\nu}(\partial\phi)^{2} + \frac{1}{2}g_{\mu\nu}V_{eff}\right)$$
$$-x\frac{V_{b}}{2}\left(F_{\mu}{}^{\rho}F_{\nu\rho} - \frac{g_{\mu\nu}}{4}F_{\rho\sigma}F^{\rho\sigma}\right) = 0, \qquad (2.11)$$

$$\frac{1}{\sqrt{-g}}\partial_{\mu}\left(\sqrt{-g}g^{\mu\nu}\partial_{\nu}\phi\right) + \frac{3}{8}\frac{\partial V_{eff}}{\partial\phi} - \frac{3x}{32}\frac{\partial V_{b}}{\partial\phi}F^{2} = 0, \qquad (2.12)$$

$$\partial_{\mu} \left(\sqrt{-g} V_b F^{\mu\nu} \right) = 0 \,, \tag{2.13}$$

respectively. Here we introduced the following combinations of potentials

$$V_b(\lambda) = V_f(\lambda)w(\lambda)^2, \qquad V_{eff}(\lambda) = V_g(\lambda) - xV_{f0}.$$
 (2.14)

We first introduce a constant background magnetic field in the U(1) part of the vector field (2.7)

$$V_{\mu} = \left(0, -\frac{x_2 B}{2}, \frac{x_1 B}{2}, 0, 0\right). \tag{2.15}$$

Then the Maxwell's equations are automatically satisfied by (2.15). Presence of this constant magnetic field in the x_3 direction breaks the SO(3) symmetry to SO(2), that is, rotations on the x_1x_2 plane. Accordingly, we choose an ansatz for the metric and the dilaton as

$$ds^{2} = e^{2A(r)} \left(-e^{g(r)} dt^{2} + dx_{1}^{2} + dx_{2}^{2} + e^{2W(r)} dx_{3}^{2} + e^{-g(r)} dr^{2} \right), \qquad \lambda = \lambda(r) \quad (2.16)$$

where $r \in [0, r_h]$. The UV boundary is at r = 0, where we demand AdS_5 asymtotics $(A \to -\log(r), g \to 0, W \to 0 \text{ as } r \to 0)$. r_h is the location of the horizon where $g(r_h) = -\infty$.

With the ansatz (2.16), the Einstein's equations (2.11) yield three second order equations for functions A(r), g(r), W(r) and one constraint equation [49]. The scalar equation of motion (2.12) is not independent and can be obtained from the Einstein equations. In practice, it can be replaced by the aforementioned first order constraint equation. All in all, one obtains the following system of differential equations of degree seven [49]

$$A'' - A'^{2} + \frac{1}{3} \left(W'' + W'^{2} \right) = -\frac{4}{9} (\phi')^{2}$$
 (2.17)

$$g'' + g'(g' + 3A' + W') = \frac{xB^2V_b}{e^{2A+g}}$$
(2.18)

$$(W'e^{3A+W+g})' = \frac{xB^2}{2}V_b e^{W+A}$$
(2.19)

$$3A'(g'+4A'+2W')+g'W'+e^{-g}V_{eff}-\frac{4}{3}(\phi')^2=-\frac{xB^2V_b}{2e^{4A+g}}.$$
 (2.20)

For the potential $V_q(\lambda)$, we choose the ihQCD potential [22, 36–38]

$$V_g(\lambda) = \frac{12}{l^2} \left(1 + V_0 \lambda + V_1 \lambda^{4/3} \sqrt{\log(1 + V_2 \lambda^{4/3} + V_3 \lambda^2)} \right), \tag{2.21}$$

with coefficients

$$V_0 = \frac{8}{9}\beta_0, \quad V_1 = 1000V_0^{\frac{4}{3}}, \quad V_3 = 100000k^2$$

$$V_2 = \left(23 + 36 \times \frac{51}{121}\right)^2 \frac{b_0}{6561V_0^2 V_1^2}$$
(2.22)

where $\beta_0 = 22/(3(4\pi)^2)$, $b_0 = 9/8$ and $k = (8/9)\beta_0$. The UV asymptotics (small λ) of this potential match the perturbative large- N_c β -function and corresponds to initial conditions of an RG flow with asymptotic freedom in the dual field theory [22]. In the IR (large λ) this form of the potential guarantees that the dual field theory is confining with a gapped glueball spectrum [36].

The flavor sector potentials $V_{f0}(\lambda)$ and $w(\lambda)$ can be determined by comparing their asymptotics with lattice and pertubative results. Following [41–44] we choose,

$$V_{f0}(\lambda) = W_0(1 + W_1\lambda + W_2\lambda^2), \tag{2.23}$$

$$w(\lambda) = \left(1 + \frac{3a_1}{4}\lambda\right)^{-\frac{4}{3}},\tag{2.24}$$

with

$$a_1 = \frac{115 - 16x}{216\pi^2}, \qquad W_0 = \frac{3}{11}, \qquad W_1 = \frac{24 + (11 - 2x)W_0}{27\pi^2W_0},$$
 (2.25)

$$W_2 = \frac{24(857 - 46x) + (4619 - 1714x + 92x^2)W_0}{46656\pi^4 W_0}. (2.26)$$

This choice of the flavor potentials are motivated by matching the perturbative anomalous dimension of the quark mass operator in the UV and the requirement of chiral symmetry and the meson spectra in the IR [44].

With this choice for the potentials, equations (2.17-2.20) can only be solved numerically. This system of equations require 7 integration constants. However, one can easily see that the regularity at the horizon fixes two of these integration constants automatically, one in (2.18) and (2.19) each. Two constants among the leftover 5 are determined by the near UV requirements $g \to 0$ and $W \to 0$. The remaining 3 integration constants are physical; they correspond to the volume of a unit cell in the dual theory, the temperature T and Λ_{QCD} . Furthermore, the volume just factors out as a multiplicative factor in all dimensionful parameters and cancels out in dimensionless ratios. Therefore, together with the magnetic field, our solutions will only be characterized by three parameters: B, T and Λ_{QCD} . These numerical solutions are first constructed in [49] by matching the background solution with B = 0 near the boundary. Here we obtain the same solutions with different temperature values in the interval $T/T_c \in [1.00208, 2.17277]$ and different magnetic field values in the interval $eB_{phys} \in [0.05978, 1.7335] GeV^2$, where T_c is the critical temperature

for the decofinement transition for B = 0 [37], e is the fundamental electric charge and we defined the "physical" magnetic field B_{phys} in the dual field theory

$$B_{phys} = \frac{B}{l^2},\tag{2.27}$$

where $l \approx \frac{0.00161482}{247 MeV}$ [49]. The black brane solutions that we obtain by solving the equations (2.17-2.20) are identical to those in [49]. Therefore we shall not show them here. Instead, we directly focus on the quasinormal mode spectrum in the next section.

3 Quasinormal mode spectra

Quasinormal modes (QNMs) are linear fluctuations around the background that satisfy infalling boundary condition at the horizon and vanishing Dirichlet boundary condition at the boundary. Therefore we first need to determine these linear fluctuation equations around the background solution (2.16) of the previous section. It is standard to take fluctuations in a plane wave form times and r-dependent function determined from the linearized Einstein and Maxwell equations. Setting the plane wave part is nontrivial for the model we consider here for the following reason. The background metric (2.16) has SO(2) symmetry around the x_3 -axis, because of the presence of a constant magnetic field along that direction. Any plane wave form other than $\exp(ikx_3 - i\omega t)$ would spoil this symmetry structure and would result in coupling between all metric and gauge field fluctuations. This general problem is very hard to solve and we leave it for future work. Instead, here we consider the case when the momentum \vec{k} is aligned with the magnetic field \vec{B} . The fluctuations we consider in this paper are then of the form

$$g_{\mu\nu} = g_{\mu\nu}^{(0)} + g_{\mu\nu}^{(1)}, \qquad V_{\mu} = V_{\mu}^{(0)} + V_{\mu}^{(1)},$$
 (3.1)

where

$$g_{\mu\nu}^{(1)} = e^{i(kx_3 - \omega t)} h_{\mu\nu}(r), \qquad V_{\mu}^{(1)} = ie^{i(kx_3 - \omega t)} v_{\mu}(r).$$
 (3.2)

Here and throughout the paper, the superscript (0) denotes background quantities and the superscript (1) denotes fluctuations. In this case we can decouple the scalar, vector, and tensor-type fluctuations. After imposing the radial gauge

$$h_{tr} = h_{x_3r} = h_{rr} = h_{r\alpha} = 0, v_r = 0,$$
 (3.3)

we end up with the classification [52]

Spin2 (scalar channel):
$$h_{\alpha\beta} - \delta_{\alpha\beta}h/2$$
 (3.4)

Spin1 (shear channel):
$$h_{t\alpha}, h_{x_3\alpha}, v_{\alpha}$$
 (3.5)

Spin0 (sound channel):
$$h_{tt}, h_{tx_3}, h_{x_3x_3}, h, v_t, v_{x_3}, \phi$$
 (3.6)

where $\alpha = x_1, x_2$ and $h = \sum_{\alpha} h_{\alpha\alpha}$.

We note that the gauge (3.3) does not completely fix the diffeomorphism invariance. Under infinitesimal diffeomorphisms, $x^{\mu} \to x^{\mu} + \xi^{\mu}$ (where $\xi_{\mu} = e^{i(kx_3 - \omega t)} \zeta_{\mu}(r)$), the metric, gauge field and dilaton fluctuations transform as

$$g_{\mu\nu}^{(1)} \to g_{\mu\nu}^{(1)} - \nabla_{\mu}^{(0)} \xi_{\nu} - \nabla_{\nu}^{(0)} \xi_{\mu}, \qquad (3.7)$$

$$V_{\mu}^{(1)} \to V_{\mu}^{(1)} - g^{(0)\tau\lambda} V_{\tau}^{(0)} \nabla_{\mu}^{(0)} \xi_{\lambda} - g^{(0)\tau\lambda} \xi_{\lambda} \nabla_{\tau}^{(0)} V_{\mu}^{(0)}, \qquad (3.8)$$

$$V_{\mu}^{(1)} \to V_{\mu}^{(1)} - g^{(0)\tau\lambda} V_{\tau}^{(0)} \nabla_{\mu}^{(0)} \xi_{\lambda} - g^{(0)\tau\lambda} \xi_{\lambda} \nabla_{\tau}^{(0)} V_{\mu}^{(0)}, \tag{3.8}$$

$$\phi^{(1)} \to \phi^{(1)} - \xi^{\mu} \nabla^{(0)}_{\mu} \phi^{(0)}. \tag{3.9}$$

In this paper we only consider the QNMs in the scalar and shear channels. In the next subsection we investigate temperature, magnetic field and momentum dependence of the scalar channel QNM spectrum. In the subsequent subsection, we perform a similar investigation for the shear channel.

3.1 Scalar channel

In this subsection, we consider fluctuations in the scalar channel (3.4),

$$g_{x_1 x_2}^{(1)} = e^{i(kx_3 - \omega t)} e^{2A(r)} H_{x_1 x_2}(r)$$
(3.10)

where $H_{x_1x_2} = h_{x_2}^{x_1}$ is invariant under the residual gauge transformation (3.7) and from now on we denote it by $Z_1(r)$. Expanding equation (2.11) to first order we obtain the gauge invariant fluctuation equation

$$Z_1''(r) + \left[3A'(r) + g'(r) + W'(r)\right]Z_1'(r) + \left[\frac{\omega^2}{e^{2g(r)}} - \frac{k^2}{e^{2W(r) + g(r)}}\right]Z_1(r) = 0. \quad (3.11)$$

We use the shooting method to determine the QNM spectrum. In this procedure we first numerically integrate (3.11) by specifying the infalling boundary condition at the horizon

$$Z_1(r_h - r) = (r_h - r)^{-\frac{i\omega}{4\pi T}} \left[a_0 + a_1(r_h - r) + \dots \right], \tag{3.12}$$

where a_1 etc. can be expressed as functions of a_0 by carrying out the near horizon expansion of (3.11). The coefficient a_0 on the other hand is arbitrary and we set it to 1. The solution should also satisfy the Dirichlet boundary condition $Z_1(0) = 0$ on the boundary. We then adjust the frequency $\omega_n = \Omega_n + i\Gamma_n$ to determine the solutions that satisfy this requirement.

Our results are displayed in the figures 1, 2 and 3. We show our results in terms of dimensionless frequency and momentum

$$\bar{\omega} = \frac{\omega}{2\pi T_c}, \qquad \bar{k} = \frac{k}{2\pi T_c}.$$
 (3.13)

In figure 1 we plot the temperature dependence of the three lowest QNMs and of a purely imaginary mode for $T/T_c \in [1.00208, 2.17277], eB_{phys} = 0.239109 GeV^2, \bar{k} = 0.001.$ We observe that the real parts increase when we heat the system up. The imaginary parts move away from the real axis and the gaps between the different modes become bigger with the increasing temperature as expected. We also observe a purely imaginary mode down on the imaginary axis displayed in figure 1(b). It never develops a real part and it

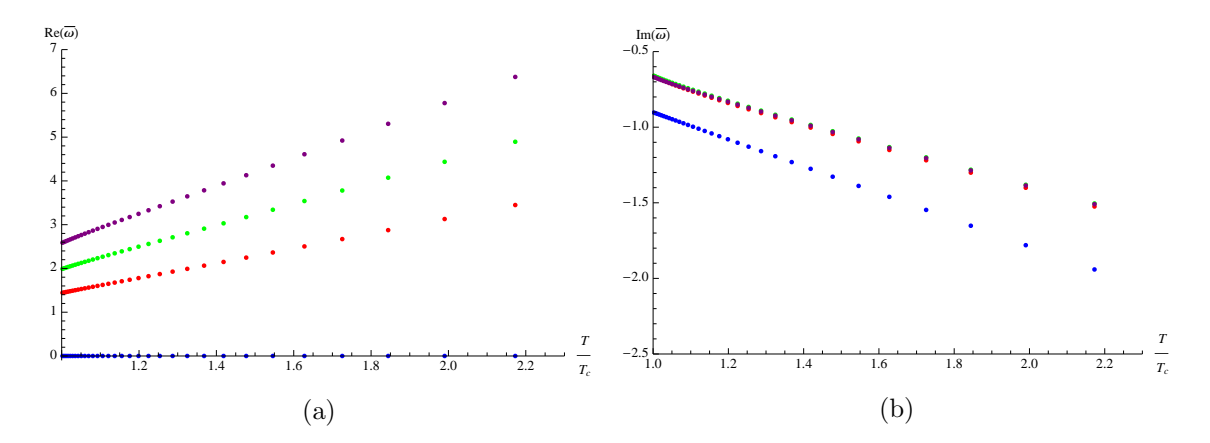


Figure 1: T-dependence of quasinormal frequencies for temperature values varying between $T/T_c \in [1.00208, 2.17277]$ and for fixed $eB_{phys} = 0.239109 GeV^2$, $\bar{k} = 0.001$: (a) the real parts and (b) imaginary parts of the three lowest modes and purely imaginary mode.

never becomes dominant at this small value of \bar{k} . With the increasing temperature, its imaginary part again moves away from the real axis.

In figure 2 we show the magnetic field dependence of the three lowest QNMs and the aforementioned purely imaginary mode for $eB_{phys} \in [0.119555, 1.73354]GeV^2, T/T_c = 1.0221$, $\bar{k} = 0.01$. The real parts slightly increase with increasing magnetic field while the imaginary parts move away from the real axis.

In figure 3 we show the momentum dependence of the three lowest QNMs and the purely imaginary mode for $\bar{k} \in [0, 20.6974]$, $T/T_c = 1.84416$, $eB_{phys} = 0.239109 GeV^2$. The real parts increase with increasing momentum. On the other hand, the momentum dependence of the imaginary parts are more complicated. Crossing occurs between each pair among the lowest three modes we consider, and this happens at a different value of momentum for each pair.

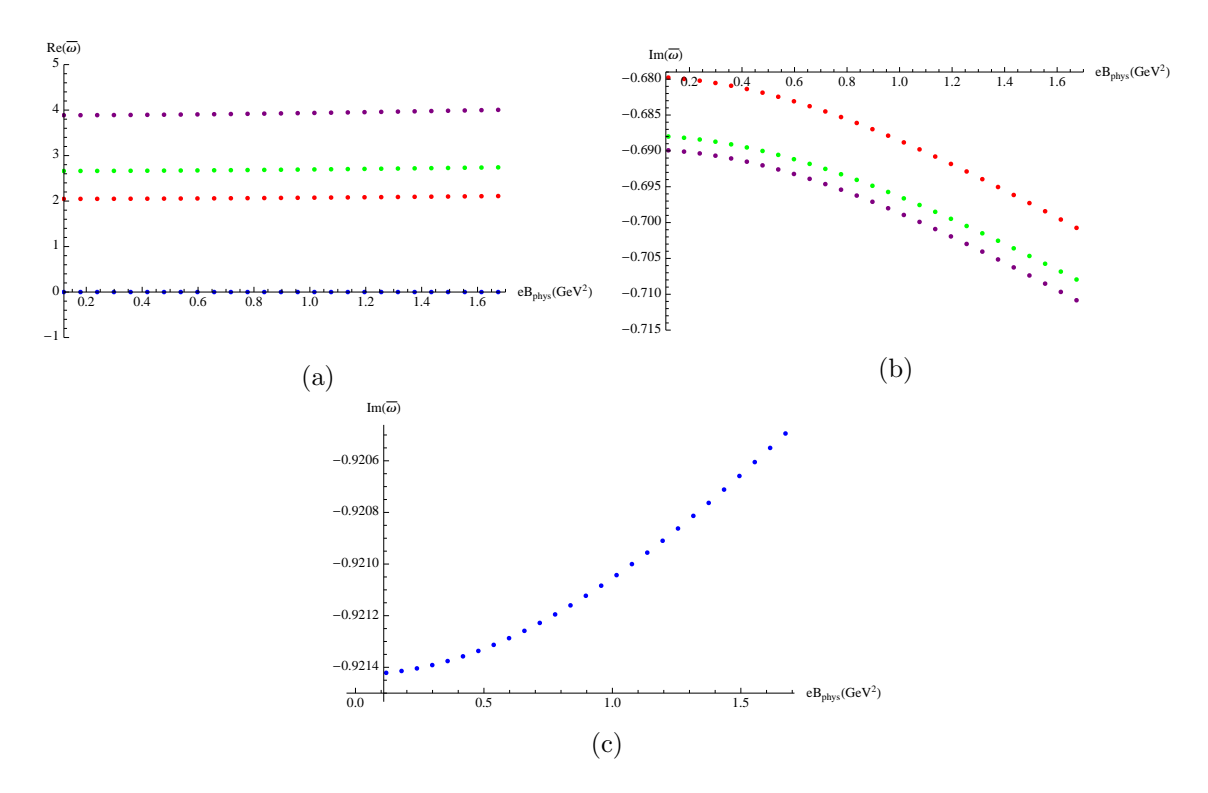


Figure 2: B-dependence of quasinormal frequencies magnetic field values varying between $eB_{phys} \in [0.119555, 1.73354] GeV^2$ and for fixed $T/T_c = 1.0221$, $\bar{k} = 0.01$: (a) the real of the three lowest and purely imaginary mode and (b) the imaginary parts the three lowest, (c) the purely imaginary mode.

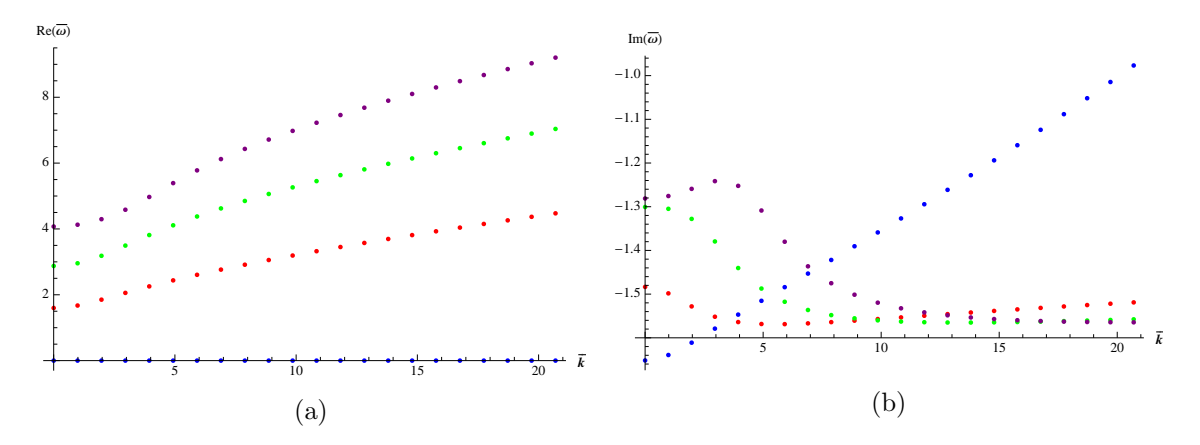


Figure 3: \bar{k} -dependence of quasinormal frequencies for momentum values varying between $\bar{k} \in [0, 20.6974]$ and for fixed $T/T_c = 1.84416$ and $eB_{phys} = 0.239109 GeV^2$: (a) the real parts and (b) the imaginary parts of the three lowest modes and the purely imaginary mode. $\bar{k}_c = 7.88472$ is the critical momentum value in which the purely imaginary mode becomes dominant.

3.2 Shear channel

Next, we consider quasinormal fluctuations in the shear channel (3.5) by turning on the fluctuations

$$g_{tx_2}^{(1)} = e^{i(kx_3 - \omega t)} e^{2A(r)} H_{tx_2}(r), \tag{3.14}$$

$$g_{x_2x_3}^{(1)} = e^{i(kx_3 - \omega t)} e^{2A(r)} H_{x_2x_3}(r), \tag{3.15}$$

$$V_{x_1}^{(1)} = ie^{i(kx_3 - \omega t)} v_{x_1}(r). \tag{3.16}$$

where $H_{tx_2} = h_{x_2}^t$, $H_{x_2x_3} = h_{x_2}^{x_3}$. Expanding equations (2.11) and (2.13) to linear order, we obtain the following system of equations

$$H_{tx_2}''(r) + \left[3A'(r) + W'(r)\right]H_{tx_2}'(r) + \left[\frac{-e^{2W(r)}k^2}{e^{g(r)}} - \frac{4B^2e^{-2A(r)}Z(\phi)}{e^{g(r)}}\right]H_{tx_2}(r)$$
$$-\frac{e^{-2W(r)}k\omega}{e^{g(r)}}H_{x_3x_2} - \frac{4Be^{2A(r)}\omega Z(\phi)}{e^{g(r)}}v_{x_1}(r) = 0,$$
(3.17)

$$H_{x_3x_2}''(r) + \left[3A'(r) + g'(r) - W'(r)\right] H_{tx_2}'(r) + \left[\frac{\omega^2}{e^{2g(r)}} - \frac{4B^2 e^{-2A(r)} Z(\phi)}{e^{g(r)}}\right] H_{x_3x_2}(r) + \frac{k\omega}{e^{g(r)}} H_{tx_2} + \frac{4Be^{2A(r)} kZ(\phi)}{e^{g(r)}} v_{x_1}(r) = 0,$$
(3.18)

$$v_{x_1}''(r) + \left(A'(r) + g'(r) + W'(r) + \frac{Z'(\phi)\phi'(r)}{Z(\phi)}\right)v_{x_1}'(r) + \left(\frac{\omega^2}{e^{2g(r)}} - \frac{e^{2W(r)}k^2}{e^{g(r)}}\right)v_{x_1}(r) + \frac{B\omega}{e^{2g(r)}}H_{tx_2}(r) + \frac{Be^{2W(r)}k}{e^{g(r)}}H_{x_3x_2}(r) = 0,$$
(3.19)

where $Z(\phi) = xV_f(\phi)w^2(\phi)/4$. In addition to these, one obtains a constraint equation

$$\frac{k}{2}H'_{x_3x_2}(r) + \frac{e^{2W(r)}\omega}{2e^{g(r)}}H'_{tx_2}(r) + 2Be^{2(W(r)-A(r))}Z(\phi)v'_{x_1}(r) = 0.$$
 (3.20)

Since we have three second order equations and a first order constraint equation, this system of differential equations can be reduced to a set of two second order equations. Considering the gauge transformations (3.7) and (3.8) one determines the gauge invariant combinations as

$$Z_2(r) = kH_{tx_2}(r) + \omega H_{x_3x_2}(r), \tag{3.21}$$

$$Z_3(r) = v_{x_1} + \frac{B}{2k\omega} [kH_{tx_2}(r) - \omega H_{x_3x_2}(r)].$$
 (3.22)

Then, from equations (3.17), (3.18), (3.19) and (3.20) we obtain two second order gauge invariant equations for Z_2 and Z_3

$$Z_2''(r) + C_1 Z_2'(r) + C_2 Z_2(r) + C_3 Z_3'(r) = 0, (3.23)$$

$$Z_3''(r) + D_1 Z_3'(r) + D_2 Z_3(r) + D_3 Z_2'(r) = 0. (3.24)$$

The coefficients C_1 , C_2 , C_3 , D_1 , D_2 and D_3 are lengthy and presented in Appendix A. To determine the QNM spectrum, we again use the shooting method. We first numerically integrate equations (3.23) and (3.24) by specifying infalling boundary conditions at the horizon

$$Z_2(r_h - r) = (r_h - r)^{-\frac{i\omega}{4\pi T}} \left[b_0 + b_1(r_h - r) + \dots \right]$$
(3.25)

$$Z_3(r_h - r) = (r_h - r)^{-\frac{i\omega}{4\pi T}} \left[c_0 + c_1(r_h - r) + \dots \right]$$
(3.26)

where b_1 , c_1 etc. can be expressed in terms of b_0 and c_0 by considering the near horizon expansion of equations (3.23) and (3.24). The coefficients b_0 and c_0 are arbitrary. We first set $b_0 \to 1$ and $c_0 \to 0$, solve equations (3.23) and (3.24) numerically and obtain the first set of linearly independent solutions $\{Z_2^{(1)}, Z_3^{(1)}\}$. We then repeat the same procedure for $b_0 \to 0$ and $c_0 \to 1$ and obtain the second set of linearly independent solutions $\{Z_2^{(2)}, Z_3^{(2)}\}$. The Dirichlet boundary condition then means that the determinant of the matrix of maximally independent solutions should vanish on the boundary:

$$\lim_{r \to r_c} \det[H] = \lim_{r \to r_c} \left[Z_2^{(1)} Z_3^{(2)} - Z_2^{(2)} Z_3^{(1)} \right] = 0, \tag{3.27}$$

where r_c is the UV-cutoff. We then adjust the frequency $\omega_n = \Omega_n + i\Gamma_n$ to determine the solutions which satisfy this requirement. Our results are shown in figures 4, 5 and 6 below. All the features we observe are very similar to the observations in the scalar channel above.

In figure 4 we plot the temperature dependence of the three lowest QNMs and one purely imaginary mode for $T/T_c \in [1.00208, 2.17277]$, $eB_{phys} = 0.239109 GeV^2$, $\bar{k} = 0.001$. The qualitative behaviour of the modes are similar to the scalar channel. The real parts increases when we heat the system up. The imaginary parts, on the other hand, move away from the real axis and the gap between different modes become larger with increasing temperature. This is the same behaviour as observed in the scalar channel and in accordance with general expectations. We observe a purely imaginary mode. It never develops a real part and it never becomes dominant for this choice of k and k. With increasing temperature, its imaginary part again moves away from the real axis.

In figure 5 we plot the magnetic field dependence of the three lowest QNMs and the purely imaginary mode for $eB_{phys} \in [0.119555, 1.73354] GeV^2, T/T_c = 1.0221, \bar{k} = 0.01$. The qualitative behaviour of the modes are again similar to the scalar channel. Their real parts all increase, except the purely imaginary mode that never develops a real part, and the imaginary parts of all the modes move down, away from the real axis in all cases.

In figure 6 we plot the momentum dependence of three lowest QNMs and the purely imaginary mode in the shear channel, for $\bar{k} \in [0, 20.6974]$, $T/T_c = 1.84416$, $eB_{phys} = 0.239109 GeV^2$. Again the qualitative features similar to the scalar channel. The real parts increase with the increasing momenta. The momentum dependence of the imaginary parts are more complicated. For each mode crossing occurs between different modes, at a certain value of the momentum as shown in figure 6 (b). We also observe that the second QNM (green curve on figure 6) bifurcates as a function of \bar{k} at $\bar{k} \approx 2$ into two QNMs. Similar behavior is observed in [33].

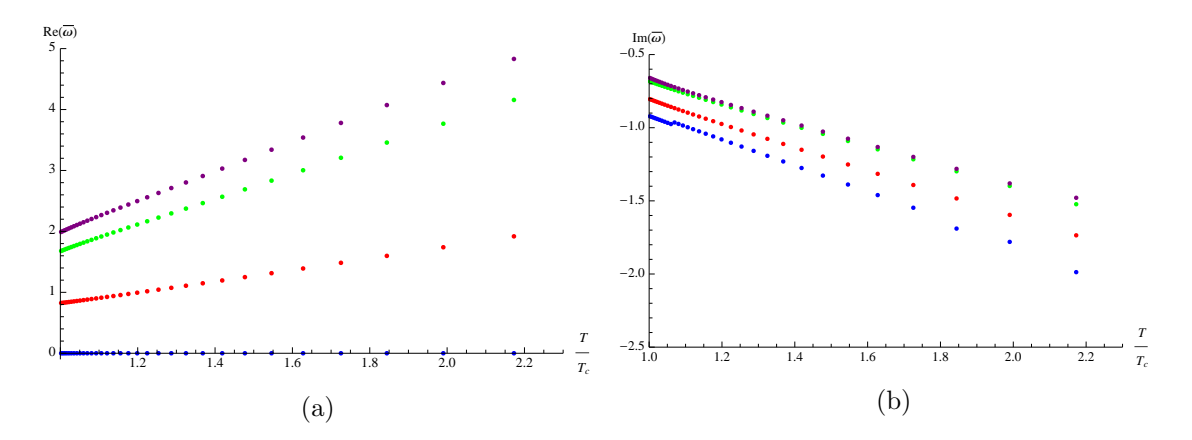


Figure 4: T-dependence of quasinormal frequencies for temperature values varying between $T/T_c \in [1.00208, 2.17277]$ and for fixed $eB_{phys} = 0.239109 GeV^2$, $\bar{k} = 0.001$: (a) the real parts and (b) imaginary parts of the three lowest modes and purely imaginary mode.

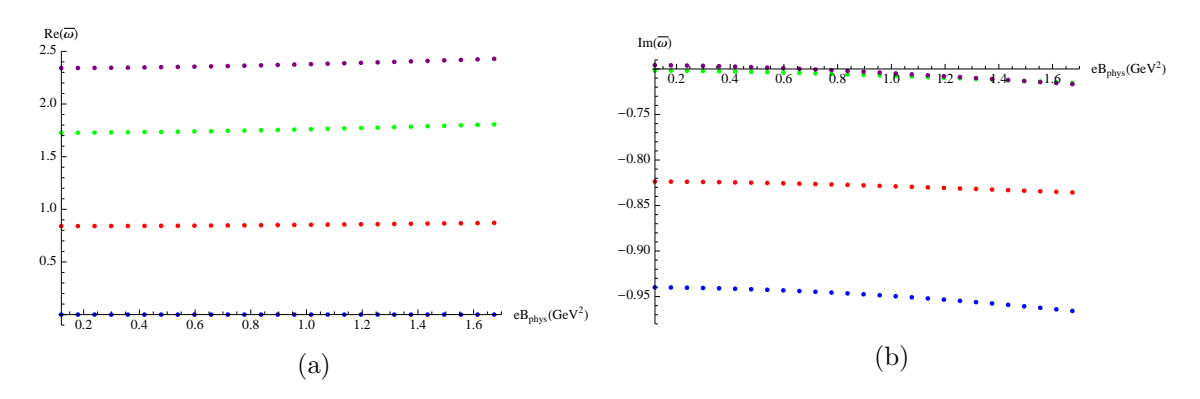


Figure 5: B-dependence of quasinormal frequencies magnetic field values varying between $eB_{phys} \in [0.119555, 1.73354] GeV^2$ and for fixed $T/T_c = 1.0221$, $\bar{k} = 0.01$: (a) the real and (b) the imaginary parts the three lowest and the purely imaginary mode.

4 Discussion

In this paper we investigate equilibration of linear fluctuations in the deconfined phase of a strongly coupled large- N_c 4D gauge theory that is confining at low temperatures. In particular we consider the case when the system is placed under an external magnetic field in the x_3 direction and we determine the location of the poles in the retarded Green's function of the stress tensor operator $T_{x_1x_2}$ (the scalar channel) and a mixture of the stress tensor components $T_{t\alpha}$, $T_{x_3\alpha}$ and the current operator J_{β} (the shear channel), where $\alpha = x_1, x_2$ and $\beta = x_2, x_1$ respectively. These poles (especially the lowest modes) control the equilibration process; in particular the equilibration time is well approximated by the imaginary part of the lowest mode $\tau \propto -1/\text{Im}\omega$. It is therefore quite interesting to determine how this spectrum depends on the parameters T, B and the momentum k, that we align with the magnetic field. We carry out this analysis using the holographic dual formulation where these poles are mapped onto the quasinormal modes of the corresponding

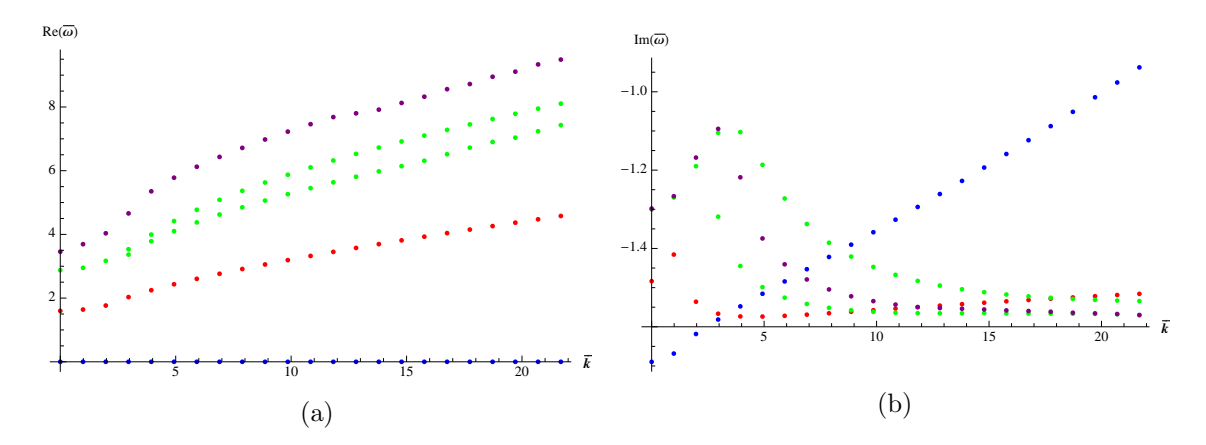


Figure 6: \bar{k} -dependence of quasinormal frequencies for momentum values varying between $\bar{k} \in [0, 20.6974]$ and for fixed $T/T_c = 1.84416$ and $eB_{phys} = 0.239109GeV^2$: (a) the real parts and (b) the imaginary parts of the three lowest modes and the purely imaginary mode. $\bar{k}_c = 8.87031$ is the critical momentum value in which the purely imaginary mode becomes dominant.

black-brane solution, which we determine using the shooting method. Our findings are summarized in the list in section 1. Here we discuss them in some detail and also provide an outlook.

Purely imaginary mode: We observe two separate classes of QNMs, one class with both real and imaginary parts and a second class that is purely imaginary. Such purely imaginary modes were also observed in charged black-brane solutions, first in [50] and further discussed in [35]. The latter paper conjectures an interpretation of such modes, proposing that these poles combine to form a branch cut on the complex frequency plane in the corresponding retarded Green's function in the limit they approach each other. This is a plausible interpretation, however, it does not seem to apply to our case since we were able to locate only one example of a purely imaginary mode, not an entire family as in [50] and [35]. Whether one can locate the entire family, and whether there exist a limit where they approach each other and form a branch-cut remains to be seen. Another difference between the aforementioned works and our case is that these purely imaginary modes only appear in the electrically charged black-brane solutions in their case, whereas we obtain such an example in the magnetically charged black brane. Physically, it corresponds to an overdamped ring down of the linear fluctuation since it does not possess any real part which would correspond to oscillations in time. These particular fluctuations were associated with backscattering of gravitational waves off the gravitational potential in [28]. It is plausible that the same interpretation holds in our case.

Our purely imaginary mode exists both in the scalar and the shear channels and it moves up on the imaginary axis with increasing momentum. It becomes dominant at a certain value of momentum whose value depends on T, very mildly on B and the particular channel chosen.

B dependence of the QNMs: Both in the scalar and the shear channels, both the real parts Re ω and the imaginary parts $-\text{Im}\,\omega$ increase with increasing B with the only exception of the purely imaginary mode in the scalar channel. This means that the corresponding linear fluctuations oscillate faster and become more damped at larger values of B. The latter means that the equilibration times τ become shorter. On the other hand, this should be related to the the thermalization times of the quark-gluon matter produced in heavy ion collisions at RHIC and LHC. One can estimate the thermalization times in the absence(presence) of B in the central(off-central) collisions by matching to the hydrodynamical simulations. One does not seem to find a substantial difference in the thermalization time of the plasma in the presence and absence of B. However, as also discussed in [35], this does not necessarily imply a contradiction with our results. This is because thermalization and equilibration are two different processes in general. Thermalization refers to a fully non-linear time-dependent evolution and equilibration—that we study in this paper—refers to ring down of linear fluctuations. Thermalization in heavy ion collisions is expected to be a wild, fully non-linear process that can also be studied holographically [23]. One of the most urgent open problems is then to work out the holographic thermalization of the plasma in the presence of magnetic fields. As to why the purely imaginary mode in the scalar channel behaves differently and approaches to the real axis with increasing B is to be understood.

Finally, another urgent open question is to determine the dependence of the linear mode spectra on B in the *confined* phase. This would directly provide the Landau levels in the gauge theory, and how they shift with B at strong coupling.

Acknowledgements

We thank Tara Drwenski, Ioannis Iatrakis, Aron Jansen, Cihan Saclioglu and Phil Szepietowski for useful discussions. T. D. thanks ITP, Utrecht university for hospitality where most of this work was completed. This work was supported, in part by the Netherlands Organisation for Scientific Research (NWO) under VIDI grant 680-47-518, and the Delta-Institute for Theoretical Physics (D-ITP) that is funded by the Dutch Ministry of Education, Culture and Science (OCW). T.D. was supported by the Scientific and Technological Research Council of Turkey (TUBITAK) under the programme 2214-A.

Coefficients in the gauge invariant variable equations of the shear channel

Explicit forms of the coefficients in the gauge invariant equations 3.23 and 3.24 are

$$C_{1} = \frac{e^{2W}(2B^{2}fx(V_{b}/4)[6fA' + f'] - e^{2A}\omega^{2}[f' + f\{3A' - W'\}])e^{2A}k^{2}f^{2}(3A' + W')}{f(-e^{2(A-W)}\omega^{2} + f[e^{2A}k^{2} + 4B^{2}e^{2W}x(V_{b}/4)])}, (A.1)$$

$$C_{2} = \frac{\omega^{2} - e^{2W}k^{2}f - 4B^{2}e^{-2A}fx(V_{b}/4)}{f^{2}}, (A.2)$$

$$C_2 = \frac{\omega^2 - e^{2W}k^2f - 4B^2e^{-2A}fx(V_b/4)}{f^2},$$
(A.2)

$$C_3 = -\frac{4Be^{2W}k\omega x(V_b/4)[f' - 2fW']}{-e^{2(A+W)}\omega^2 + f[e^{2A}k^2 + 4B^2e^{2W}x(V_b/4)]},$$
(A.3)

$$D_{1} = \frac{e^{2A}k^{2}f(x(V_{b}/4)[f' + f\{A' + W'\}] + fx(V'_{b}/4)\phi' + e^{2W}[2B^{2}fx^{2}(V_{b}/4)^{2}\{6fA' + f'\}])}{fx(V_{b}/4)[-e^{2(A+W)}\omega^{2} + f(e^{2A}k^{2} + 4B^{2}e^{2W}x(V_{b}/4))]}$$

$$+\frac{e^{2A}k^2f(-e^{2A}\omega^2[x(V_b/4)\{f'+f(A'+W')\}+fx(V_b'/4)\phi'])}{fx(V_b/4)[-e^{2(A+W)}\omega^2+f(e^{2A}k^2+4B^2e^{2W}x(V_b/4))]},$$
(A.4)

$$D_2 = \frac{\omega^2 - e^{-2W}k^2f - 4B^2e^{-2A}fx(V_b/4)}{f^2},$$
(A.5)

$$D_{3} = \frac{-2B^{3}e^{2W}x^{2}(V_{b}/4)^{2}[f'-2fW']}{2k\omega x(V_{b}/4)[-e^{2(A+W)}\omega^{2} + f\{e^{2A}k^{2} + 4B^{2}e^{2W}x(V_{b}/4)\}]} + \frac{Be^{2A}[x(V_{b}/4)(k^{2}\{2fA'-f'\} + 2e^{2W}\omega^{2}\{A'-W'\}) - x(V'_{b}/4)\phi'(e^{2W}\omega^{2} + k^{2}f)]}{2k\omega x(V_{b}/4)[-e^{2(A+W)}\omega^{2} + f\{e^{2A}k^{2} + 4B^{2}e^{2W}x(V_{b}/4)\}]}$$
(A.6)

where $f = \log q$, $\phi = \log \lambda$ and the derivatives of V_b are with respect to ϕ .

References

- [1] V. P. Gusynin, V. A. Miransky and I. A. Shovkovy, Dimensional reduction and catalysis of dynamical symmetry breaking by a magnetic field, Nucl. Phys. **B462** (1996) 249–290, [hep-ph/9509320].
- [2] V. Skokov, A. Yu. Illarionov and V. Toneev, Estimate of the magnetic field strength in heavy-ion collisions, Int. J. Mod. Phys. A24 (2009) 5925-5932, [0907.1396].
- [3] D. E. Kharzeev, L. D. McLerran and H. J. Warringa, The Effects of topological charge change in heavy ion collisions: 'Event by event P and CP violation', Nucl. Phys. A803 (2008) 227-253, [0711.0950].
- [4] K. Fukushima, D. E. Kharzeev and H. J. Warringa, The Chiral Magnetic Effect, Phys. Rev. **D78** (2008) 074033, [0808.3382].
- [5] U. Gursoy, D. Kharzeev and K. Rajagopal, Magnetohydrodynamics, charged currents and directed flow in heavy ion collisions, Phys. Rev. C89 (2014) 054905, [1401.3805].
- [6] K. Tuchin, Synchrotron radiation by fast fermions in heavy-ion collisions, Phys. Rev. C82 (2010) 034904, [1006.3051].
- [7] V. Voronyuk, V. D. Toneev, W. Cassing, E. L. Bratkovskaya, V. P. Konchakovski and S. A. Voloshin, (Electro-)Magnetic field evolution in relativistic heavy-ion collisions, Phys. Rev. C83 (2011) 054911, [1103.4239].

- [8] W.-T. Deng and X.-G. Huang, Event-by-event generation of electromagnetic fields in heavy-ion collisions, Phys. Rev. C85 (2012) 044907, [1201.5108].
- [9] K. Tuchin, Particle production in strong electromagnetic fields in relativistic heavy-ion collisions, Adv. High Energy Phys. **2013** (2013) 490495, [1301.0099].
- [10] L. McLerran and V. Skokov, Comments About the Electromagnetic Field in Heavy-Ion Collisions, Nucl. Phys. A929 (2014) 184–190, [1305.0774].
- [11] D. E. Kharzeev, K. Landsteiner, A. Schmitt and H.-U. Yee, 'Strongly interacting matter in magnetic fields': an overview, Lect. Notes Phys. 871 (2013) 1–11, [1211.6245].
- [12] J. Casalderrey-Solana, H. Liu, D. Mateos, K. Rajagopal and U. A. Wiedemann, Gauge/String Duality, Hot QCD and Heavy Ion Collisions, 1101.0618.
- [13] J. M. Maldacena, The Large N limit of superconformal field theories and supergravity, Int. J. Theor. Phys. 38 (1999) 1113-1133, [hep-th/9711200].
- [14] S. S. Gubser, I. R. Klebanov and A. M. Polyakov, Gauge theory correlators from noncritical string theory, Phys. Lett. B428 (1998) 105–114, [hep-th/9802109].
- [15] E. Witten, Anti-de Sitter space and holography, Adv. Theor. Math. Phys. 2 (1998) 253-291, [hep-th/9802150].
- [16] E. Witten, Anti-de Sitter space, thermal phase transition, and confinement in gauge theories, Adv. Theor. Math. Phys. 2 (1998) 505–532, [hep-th/9803131].
- [17] S. S. Gubser, Dilaton driven confinement, hep-th/9902155.
- [18] T. Sakai and S. Sugimoto, Low energy hadron physics in holographic QCD, Prog. Theor. Phys. 113 (2005) 843–882, [hep-th/0412141].
- [19] J. Erlich, E. Katz, D. T. Son and M. A. Stephanov, QCD and a holographic model of hadrons, Phys. Rev. Lett. 95 (2005) 261602, [hep-ph/0501128].
- [20] C. P. Herzog, A Holographic Prediction of the Deconfinement Temperature, Phys. Rev. Lett. 98 (2007) 091601, [hep-th/0608151].
- [21] C. Csaki and M. Reece, Toward a systematic holographic QCD: A Braneless approach, JHEP 05 (2007) 062, [hep-ph/0608266].
- [22] U. Gursoy and E. Kiritsis, Exploring improved holographic theories for QCD: Part I, JHEP 02 (2008) 032, [0707.1324].
- [23] P. M. Chesler and L. G. Yaffe, Horizon formation and far-from-equilibrium isotropization in supersymmetric Yang-Mills plasma, Phys. Rev. Lett. 102 (2009) 211601, [0812.2053].
- [24] P. M. Chesler and L. G. Yaffe, Holography and colliding gravitational shock waves in asymptotically AdS₅ spacetime, Phys. Rev. Lett. 106 (2011) 021601, [1011.3562].
- [25] M. P. Heller, R. A. Janik and P. Witaszczyk, The characteristics of thermalization of boost-invariant plasma from holography, Phys. Rev. Lett. 108 (2012) 201602, [1103.3452].
- [26] M. P. Heller, D. Mateos, W. van der Schee and D. Trancanelli, Strong Coupling Isotropization of Non-Abelian Plasmas Simplified, Phys. Rev. Lett. 108 (2012) 191601, [1202.0981].
- [27] D. T. Son and A. O. Starinets, Minkowski space correlators in AdS / CFT correspondence: Recipe and applications, JHEP **09** (2002) 042, [hep-th/0205051].
- [28] E. Berti, V. Cardoso and A. O. Starinets, Quasinormal modes of black holes and black branes, Class. Quant. Grav. 26 (2009) 163001, [0905.2975].

- [29] U. Gursoy, S. Lin and E. Shuryak, Instabilities near the QCD phase transition in the holographic models, Phys. Rev. D88 (2013) 105021, [1309.0789].
- [30] A. Buchel, M. P. Heller and R. C. Myers, Equilibration rates in a strongly coupled nonconformal quark-gluon plasma, Phys. Rev. Lett. 114 (2015) 251601, [1503.07114].
- [31] R. A. Janik, G. Plewa, H. Soltanpanahi and M. Spalinski, *Linearized nonequilibrium dynamics in nonconformal plasma*, *Phys. Rev.* **D91** (2015) 126013, [1503.07149].
- [32] T. Ishii, E. Kiritsis and C. Rosen, Thermalization in a Holographic Confining Gauge Theory, JHEP 08 (2015) 008, [1503.07766].
- [33] R. A. Janik, J. Jankowski and H. Soltanpanahi, Quasinormal modes and the phase structure of strongly coupled matter, 1603.05950.
- [34] U. Gursoy, A. Jansen and W. van der Schee, A new dynamical instability in Anti-de-Sitter spacetime, 1603.07724.
- [35] S. Janiszewski and M. Kaminski, Quasinormal modes of magnetic and electric black branes versus far from equilibrium anisotropic fluids, Phys. Rev. **D93** (2016) 025006, [1508.06993].
- [36] U. Gursoy, E. Kiritsis and F. Nitti, Exploring improved holographic theories for QCD: Part II, JHEP 02 (2008) 019, [0707.1349].
- [37] U. Gursoy, E. Kiritsis, L. Mazzanti and F. Nitti, *Holography and Thermodynamics of 5D Dilaton-gravity*, *JHEP* **05** (2009) 033, [0812.0792].
- [38] U. Gursoy, E. Kiritsis, L. Mazzanti and F. Nitti, *Improved Holographic Yang-Mills at Finite Temperature: Comparison with Data*, *Nucl. Phys.* **B820** (2009) 148–177, [0903.2859].
- [39] R. Casero, E. Kiritsis and A. Paredes, Chiral symmetry breaking as open string tachyon condensation, Nucl. Phys. B787 (2007) 98–134, [hep-th/0702155].
- [40] I. Iatrakis, E. Kiritsis and A. Paredes, An AdS/QCD model from tachyon condensation: II, JHEP 11 (2010) 123, [1010.1364].
- [41] M. Jarvinen and E. Kiritsis, Holographic Models for QCD in the Veneziano Limit, JHEP 03 (2012) 002, [1112.1261].
- [42] T. Alho, M. Jarvinen, K. Kajantie, E. Kiritsis and K. Tuominen, On finite-temperature holographic QCD in the Veneziano limit, JHEP 01 (2013) 093, [1210.4516].
- [43] D. Arean, I. Iatrakis, M. Jrvinen and E. Kiritsis, V-QCD: Spectra, the dilaton and the S-parameter, Phys. Lett. B720 (2013) 219–223, [1211.6125].
- [44] D. Arean, I. Iatrakis, M. Jrvinen and E. Kiritsis, The discontinuities of conformal transitions and mass spectra of V-QCD, JHEP 11 (2013) 068, [1309.2286].
- [45] T. Alho, M. Jrvinen, K. Kajantie, E. Kiritsis, C. Rosen and K. Tuominen, A holographic model for QCD in the Veneziano limit at finite temperature and density, JHEP 04 (2014) 124, [1312.5199].
- [46] M. Jarvinen, Massive holographic QCD in the Veneziano limit, JHEP 07 (2015) 033, [1501.07272].
- [47] S. W. Hawking and D. N. Page, Thermodynamics of Black Holes in anti-De Sitter Space, Commun. Math. Phys. 87 (1983) 577.
- [48] R. Rougemont, R. Critelli and J. Noronha, *Holographic calculation of the QCD crossover temperature in a magnetic field*, *Phys. Rev.* **D93** (2016) 045013, [1505.07894].

- [49] T. Drwenski, U. Gursoy and I. Iatrakis, *Thermodynamics and CP-odd transport in Holographic QCD with Finite Magnetic Field*, 1506.01350.
- [50] K. Maeda, M. Natsuume and T. Okamura, Viscosity of gauge theory plasma with a chemical potential from AdS/CFT, Phys. Rev. D73 (2006) 066013, [hep-th/0602010].
- [51] E. D'Hoker and P. Kraus, Magnetic Brane Solutions in AdS, JHEP 10 (2009) 088, [0908.3875].
- [52] P. K. Kovtun and A. O. Starinets, Quasinormal modes and holography, Phys. Rev. D72 (2005) 086009, [hep-th/0506184].